Biol Cybern (2016) 110:41–53
DOI 10.1007/s00422-015-0676-0

ORIGINAL ARTICLE

Biological Cybernetics

The coordination dynamics of mobile conjugate reinforcement

J. A. Scott Kelso[1,2] · **Armin Fuchs**[1,3]

Received: 13 July 2015 / Accepted: 15 December 2015 / Published online: 12 January 2016

Abstract What we know about infant learning and memory is founded largely on systematic studies by the late Carolyn Rovee-Collier (1942–2014) and her associates of a phenomenon called mobile conjugate reinforcement. Experiments show that when a ribbon is attached from a 3-month-old infant's foot to a mobile suspended overhead the baby quickly realizes it can make the mobile move. The mobile, which offers interesting sights and sounds, responds conjugately to the baby's vigorous kicks which increase in rate by a factor of 3–4. In this paper, using the concepts, methods and tools of coordination dynamics, we present a theoretical model which reproduces the experimental observations of Rovee-Collier and others and predicts a number of additional features that can be experimentally tested. The model is a dynamical system consisting of three equations, one for the baby's leg movements, one for the jiggling motion of the mobile and one for the functional coupling between the two. A key mechanism in the model is positive feedback which is shown to depend sensitively on bifurcation parameters related to the infant's level of attention and inertial properties of the mobile. The implications of our model for the dynamical (and developmental) origins of agency are discussed.

✉ J. A. Scott Kelso
kelso@ccs.fau.edu

✉ Armin Fuchs
afuchs@fau.edu

[1] Center for Complex Systems and Brain Sciences, Florida Atlantic University, 777 Glades Road, Boca Raton, FL 33431, USA

[2] Intelligent Systems Research Centre, Ulster University, Derry ~ Londonderry BT48 7JL, Northern Ireland

[3] Department of Physics, Florida Atlantic University, 777 Glades Road, Boca Raton, FL 33431, USA

Keywords Mobile conjugate reinforcement · Infant development · Dynamical systems · Self-organization · Agency · Positive feedback

1 Introduction

In 1969 Rovee and Rovee introduced a novel experimental paradigm into the study of infant development that they called mobile conjugate reinforcement. The paradigm was carried out on 18 healthy and apparently normal infants ranging in age from 9 to 12 weeks and consisted of three phases (Fig. 1). The first and third phases were baseline conditions in which the supine baby's leg movements were recorded as he/she simply observed a brightly colored mobile located directly overhead, the main features of which were 7–10 wooden figures that if shook moved and made a noise. In the key second testing or acquisition phase, a silk cord was looped around the baby's ankle and hooked without slack to an overhead bar from which the mobile was suspended. Conjugate reinforcement refers to the fact that any foot or leg movements caused the mobile to move, the latter producing feedback to the baby that may play a potentially reinforcing role. Although the motion of the mobile was not measured, the idea was that the greater the force or rate of the baby's kicking[1] the more effective should be the visual and auditory feedback from the mobile's movements and colliding wooden figures. In the authors' words: "... effectively more intense responding produced a more intense reward" (Rovee and Rovee 1969, p. 35). Remarkably, in the first 5 min of such conjugate reinforcement, the response rate of foot thrusts tripled relative to

[1] Various words are used to describe the baby's leg movements, such as "foot thrusts," "kicking" and so forth. In actual fact, the baby moves its legs (quasi-)rhythmically and the usual quantities of phase, amplitude and frequency are applicable.

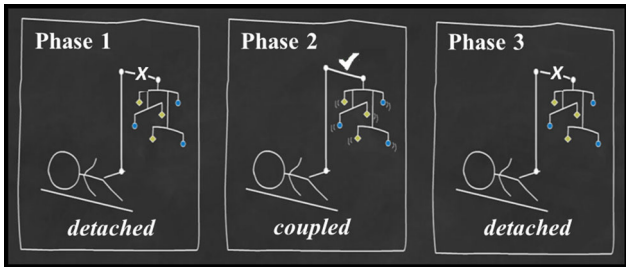

Fig. 1 Three phases of the experiment (see text for details)

control infants who were presented with identical but non-contingent auditory, visual and kinesthetic stimulation (cord attached).

A plethora of studies addressing a broad range of issues followed this discovery, including many by Rovee and her collaborators. For example, 3-month-old infants who received visual conjugate reinforcement using movement of the right leg exhibited complete reversal of leg dominance when control of mobile movement was shifted to the other leg (Rovee-Collier et al. 1978). This was an early demonstration of topographical response differentiation and functional equivalence in young infants. Using a more refined biofeedback system, Angulo-Kinzler (2001) found that infants were able to discover and produce highly specific hip and knee movements that differed in duration and direction provided they were accompanied by mobile movement and sound. She interpreted the continuous information flow generated by the movement and sound of the mobile along with proprioception from self-generated movement as central to exploratory and selection processes (see also Angulo-Kinzler et al. 2002). The control that infants gain of such reinforcing consequences is deemed to play a motivating role (Rovee-Collier and Gekoski 1979).

Similar results have emerged from other laboratories. Chen et al. (2002) used a procedure in which intralimb kicking patterns—not typically in the infant's repertoire—were differentiated on the basis of contact or no contact with a touch pad that triggered mobile movement. Whether an ankle weight was added or not, 4-month-old infants were able to successfully learn novel intralimb movements. In related work, Sargent et al. (2014) had 3-month-old infants learn, through discovery, the contingency between leg action and mobile activation. Their main goal was to study the various strategies that infants might use to make the transition from spontaneous movement to task-specific action (see also Thelen and Fisher 1983). Results suggested that infants can change coordination patterns as long as they provide a means of eliciting an interesting sensory experience, namely activation of the mobile. In short, the mobile conjugate reinforcement paradigm has played a key role in efforts to understand how infants discover and learn new patterns of behavior. Moreover, since its introduction, MCR has been employed as a key paradigm to investigate the nature of infant memory, including storage, retrieval and categorization processes and their possible neural underpinnings (Thelen and Smith 1994; Mullally and Maguire 2014).

2 Theoretical background: coordination dynamics

In the present paper, a theoretical model of mobile conjugate reinforcement is presented. Our model is based on the concepts, methods and tools of coordination dynamics, a theoretical and empirical framework aimed at understanding the coordinated behavior of living things on several levels of description (Fuchs 2013; Fuchs and Jirsa 2008; Kelso 1995, 2009; Kelso and Haken 1995; Kelso et al. 2013). In the last 30 years or so, basic principles of coordination dynamics have been shown to govern patterns of coordination: (a) within a single moving limb and between multiple moving limbs; (b) between the articulators during speech production; (c) between limb movements and tactile, visual and auditory stimuli; (d) between people interacting with each other spontaneously or intentionally; (e) between humans and other species such as riding a horse; and (f) even between humans and virtual partners realized by machines in the so-called human dynamic clamp (Dumas et al. 2014). Since their original discovery in experiments (Kelso 1981, 1984) and consequent theoretical modeling (Haken et al. 1985; Kelso et al. 1990; Schöner et al. 1986), manifold dynamical phenomena typical of pattern formation and self-organization in nonlinear dynamical systems, such as low dimensionality, multi- and meta-stable states, instabilities, phase transitions, intermittency, symmetry breaking, have been observed and often modeled in processes such as multifrequency coordination (e.g., DeGuzman and Kelso 1991), parametric stabilization (e.g., Assisi et al. 2005), trajectory formation (e.g., Buchanan et al. 1996), recruitment of new degrees of freedom (e.g., Fink et al. 2000), postural stabilization (e.g., Bardy et al. 1999), pattern recognition (e.g., Haken et al. 1990), learning (e.g., Kostrubiec et al. 2012), handwriting (e.g., Perdikis et al. 2011) and intentional behavioral change (e.g., DeLuca et al. 2010). Experiments and theory have been extended to handle not only rhythmical behaviors (e.g., Jeka et al. 1993; Schöner and Kelso 1988) but also discrete movement generation (e.g., Fink et al. 2009; Jirsa and Kelso 2005). Sophisticated time series measures (e.g., Eisenhammer et al. 1991; Chen et al. 1997) and dynamical modeling, e.g., structured flows on manifolds (Huys et al. 2014), have been used to investigate the coordination among multiple parts at multiple levels of description, including cellular/neural, muscle-joint, EMG, kinematic, biomechanical, brain (e.g., EEG, MEG, fMRI), hyperscanning (Kelso et al. 2013). Moreover, crucial predictions of theoretical models connected to critical phenomena such as critical slowing

down and critical fluctuations have been empirically tested and validated at both behavioral/cognitive and neural/brain levels (see Plenz and Niebur 2014).

A key focus of coordination dynamics is to identify collective or coordination variables and their (typically nonlinear) dynamics. Collective variables are relational quantities that are created by the cooperation or coupling among the individual parts of a system and that in turn may govern the behavior of the parts. Like the concept of order parameter in physics (cf. Haken 1978, 1983), collective variables are low-dimensional descriptions of complex systems. However, in coordination dynamics which deals with the functional and task-specific ordering among a system's many parts, collective variables are not given a priori but have to be found empirically. In numerous studies of coordination in both laboratory and real-life settings (e.g., Howard et al. 2009), collective variables have been shown to take the form of relational quantities that span interactions within the body, between the body and the environment and even between bodies themselves. In all these cases, the coupling is not (or not only) mechanical but rather informational; mutual information exchange and bidirectional coupling between parts and processes have been demonstrated to be a key aspect of biological coordination (see, e.g., Kelso et al. 2013). The governing dynamics may be said to correspond to emergent, higher-order rules that cut across different systems, different levels and different processes (Kelso 1995; Laughlin and Pines 2000; Turvey and Carello 2012). Interestingly, the concepts, methods and tools of self-organizing coordination dynamics were introduced as a research strategy into the field of motor development in the 1980s (e.g., Thelen et al. 1987a) and drove the dynamical systems approach to cognition and cognitive development (e.g., Chemero 2011; Port and van Gelder 1995; Thelen and Smith 1994). As stressed by Thelen and Smith (1994), dynamic systems have been used as a "powerful conceptual metaphor" to understand ontogenetic changes that occur in development. Although Thelen and Smith (1994, Fig. 7.3) depict the process of mobile conjugate reinforcement in terms of an ontogenetic landscape containing hypothetical "attractors" for the mobile and "context" and interpret this in terms of Edelman's (1987) theory of neuronal group selection, the difficult work of identifying laws and mechanisms has not been done. Here, we provide a quantitative model of the basic phenomenon of infant conjugate reinforcement that includes component processes and their coupling that not only reproduces the experimentally observed facts but suggests an underlying mechanism for the emergence of self-motion. In this respect, we are inspired by the work of Maxine Sheets-Johnstone (2011, p. 118) who views spontaneous movement (the baby's "kicking") as the constitutive source of agency (see also Kelso 2002). The present work suggests a modest extension, namely that the basis of causal agency is the "eureka effect," viewed here as a kind of phase transition that the baby experiences when its kicks control an environmental event, here the jiggling of the mobile.

3 The model

Beginning with Rovee and Rovee (1969), all the studies on mobile conjugate reinforcement emphasize that infants, as a result of recognizing the correspondence between their own movements and the motion of the mobile, increase their kick frequency to keep the mobile moving. In a first step, we introduce two oscillators, one for the back and forth movements of the baby's leg and one for the movement of the mobile together with a suitable dynamics for a parameter in the baby oscillator that allows for controlling its frequency.

3.1 The baby

Human rhythmic movements in adults have been studied in detail and shown to possess a number of basic features characteristic of limit cycle oscillators (Haken et al. 1985; Kay et al. 1987, 1991; Kelso et al. 1981; Beek et al. 1996). In all cases, specific modeling has been informed by experimental evidence. For example, Kay et al. (1987) following the suggestion put forth in the Haken–Kelso–Bunz (HKB) model studied experimentally the kinematic and phase portrait characteristics of simple rhythmical movements, finding excellent agreement with a hybrid model that included van-der-Pol and Rayleigh terms. Not only was a good quantitative match between model and data obtained, essential qualitative properties such as parametric changes in the shape of phase plane trajectories were found too.

Stable limit cycles are isolated closed orbits in phase space that attract nearby trajectories on the in- and outside; i.e., if the trajectory is perturbed it returns to its original orbit. This is precisely what happens when rhythmic movements in humans (or animals) are perturbed and it is one reason why limit cycles have been used extensively in neural and behavioral models of human and animal movements over the last several decades (e.g., Ajallooeian et al. 2013; Beek et al. 1995, 1996; Eisenhammer et al. 1991; Ijspeert et al. 2013a,b). Moreover, because of their stability properties, limit cycle oscillators have been employed as dynamic movement primitives in robotics applications (e.g., Raibert 1986; Ijspeert et al. 2013b). In human experiments, Kay et al. (1991) used transient mechanical perturbations to perturb the limb off its limit cycle to calculate attractor strength, accompanied by phase response analysis, Fourier spectra and calculations of correlation dimension. No biological rhythmic movements are perfectly periodic and all exhibit variability. Nevertheless, the data supported the limit cycle model, though small deviations were also noted which might imply a nonautonomous component (see also Beek et al. 2002; Fuchs et al. 2000;

Jirsa et al. 1998). Despite this caveat, Huys et al. (2014) in a recent extensive critical review of the literature covering very many studies up to the present time, conclude that despite some minor modifications "the two-dimensional limit cycle approximation accounts for most experimentally observed phenomena, which justifies their (continued) use as building blocks in the HKB model" (p. 306). Huys et al. (2014) go on to illustrate their "structured flows on manifolds" (SFM) concept by showing how the four-dimensional space spanned by the HKB model may be represented by a single limit cycle, i.e., as a phase flow in a low-dimensional subspace of a high-dimensional dynamical system.

Although not explicitly modeled, extensive experimental studies have been performed by Thelen and colleagues on supine kicking in infants (see, e.g., Jensen et al. 1989; Thelen and Fisher 1983; Thelen et al. 1981, 1987b). For typical 3-month-olds, the age group used in Rovee's experiments on mobile conjugate reinforcement, exemplar movement kinematics of hip, knee and ankle joints (e.g., in Thelen and Fisher 1983) and phase plane trajectories (e.g., Jensen et al. 1989) were found to be strongly reminiscent of limit cycle behavior. As Thelen and Smith (1994) remark, "the high dimensionality of infant kicking is condensed to produce a movement of far fewer degrees of freedom ... The cyclic trajectories of the movement act like a stable attractor (although this has not been rigorously tested) so that there is topographical similarity in the collective variables of kick displacement vs. velocity" (p. 81). In the case of mobile conjugate reinforcement, experiments show that the amplitude of the baby's kicks stays relatively constant and only the kick frequency changes. As a minimum description, this suggests a van-der-Pol term for a stable limit cycle and a Duffing term to change the frequency. The effects of these nonlinearities are well known (Fuchs 2013), and they offer a constructive way to handle mathematically what babies actually do, i.e., almost periodic kicking with an increase in rate when the mobile moves. Thus, for modeling the baby's kicks, we use a van-der-Pol oscillator with an additional Duffing term of the form

$$\ddot{x} + \dot{x}\underbrace{\{\gamma + \alpha x^2\}}_{\tilde{\gamma}} + x\underbrace{\{\omega_0^2 + \delta x^2\}}_{\omega^2} = 0 \tag{1}$$

where $\tilde{\gamma}$ represents a nonlinear damping term, which leads to a stable limit cycle for $\gamma < 0$ and $\alpha > 0$ with peak amplitude x_m

$$x_m = 2r \quad \text{with} \quad r = \sqrt{-\frac{\gamma}{\alpha}} \tag{2}$$

The frequency is determined by ω_0 and, due to the Duffing term δx^2, depends on the amplitude. Explicitly, the angular velocity ω can be approximated by

$$\omega^2 = \omega_0^2 + 3\delta r^2 = \omega_0^2 - 3\delta\frac{\gamma}{\alpha} \tag{3}$$

The square of the angular velocity, ω^2, increases linearly with δ, with α and γ kept fixed.

3.2 The mobile

The mobile is a complex moving stimulus that becomes more attractive when the infant moves it. Without the driving force of the baby's kicks, the mobile may be represented by a damped harmonic oscillator

$$\ddot{y} + \epsilon\dot{y} + \Omega_0^2 y = cx(t) \tag{4}$$

Because the baby and the mobile are connected by a ribbon without slack, a linear coupling is the simplest and best reflects the physics of the situation. Of course the coupling here is not just mechanical. The pull of the tether is directly sensed by the baby and likely amplifies the haptic and kinesthetic information that arises when the baby moves. Also several studies have shown that causal interaction can be produced without the physical connection (cf. Sect. 1), indicating that the coupling is essentially informational. For present purposes, in the spirit of Occam's razor, we stick to the simplest (linear) form of coupling that works (see also Sect. 6).

In the first and third phase of the experiment, the baby is not connected to the mobile leading to $c = 0$. Even though the dynamics of the mobile was not measured in any quantitative way—to our knowledge in any of the experiments to date—it is clear from the verbal description in Rovee and Rovee (1969) that its amplitude increased with an increasing rate of kicks as will be discussed in more detail later on.

A damped harmonic system like (4) oscillates at the frequency of the driver (after a short transient), and its amplitude depends on the eigenfrequency Ω_0, damping ϵ, driving frequency ω and amplitude x_m in a well-known way for systems showing resonance

$$y_m^2 = \frac{c^2 x_m^2}{(\Omega_0^2 - \omega^2)^2 + \epsilon^2\omega^2} \tag{5}$$

The maximum amplitude for fixed coupling c and driving x_m occurs when the denominator in (5) has a minimum or

$$\begin{aligned} &\frac{\mathrm{d}}{\mathrm{d}\omega}\{(\Omega_0^2 - \omega^2)^2 + \epsilon^2\omega^2\} \\ &\quad = -4\omega(\Omega_0^2 - \omega^2) + 2\epsilon^2\omega = 0 \\ &\quad \rightarrow \quad \omega_m = \sqrt{\Omega_0^2 - \frac{1}{2}\epsilon^2} \end{aligned} \tag{6}$$

Moreover, there is a well-determined shift between the phase of the driver and the driven system given by

$$\phi = \arctan\frac{\epsilon\omega}{\Omega_0^2 - \omega^2} \tag{7}$$

i.e., for $\omega \ll \Omega_0$ the two oscillators are in phase, whereas for $\omega = \Omega_0$ there is a phase shift of 90°.

3.3 Conjugate reinforcement

The most important aspect of the conjugate reinforcement paradigm is that the mobile responds in a time-locked fashion to the baby's leg movements. The faster the babies kick, the more motion and sound they produce. The more motion and sound produced, the more the babies kick. Experiments show that when a baby is coupled to the mobile and "realizes" that it causes mobile movement, kicking rate increases by a factor 3 to 4. In the model, this change in the kick frequency is realized by an increase in the parameter δ in (1) driven by the mobile oscillator y with a dynamics described by

$$\dot{\delta} = ay^2 - \kappa\delta \tag{8}$$

The interpretation of a and κ in (8) is pretty straight-forward: a may be viewed as a key parameter because it serves to couple the mobile and the baby. All the studies on mobile conjugate reinforcement agree that in 3-month-olds the infant's attention is captured by the motion of the mobile itself, with its salient visual and auditory features. The parameter a reflects the tight linkage of the latter to kinesthetic information generated by vigorous leg movements and the haptic coupling between the tether and the mobile. κ limits the increase and leads to the decay in rate when the baby and the mobile become decoupled. Without the driving, δ decays exponentially. This closes the circle of interactions between the baby being coupled to the mobile and the motion of the mobile caused by the baby changing its actions.

3.4 Quantitative simulation of conjugate reinforcement

The dynamical system to model conjugate reinforcement as described by Rovee and Rovee (1969) and others (see Sect. 1) consists of three equations, one for the baby's leg movements, one for the motion of the mobile and one for the coordination between the two.

$$\ddot{x} + \dot{x}\{\gamma + \alpha x^2\} + x\{\omega_0^2 + \delta x^2\} = 0 \tag{9}$$

$$\ddot{y} + \epsilon\dot{y} + \Omega_0^2 y = cx \tag{10}$$

$$\dot{\delta} = ay^2 - \kappa\delta \tag{11}$$

We first show that the model can reproduce the experimental findings and provide a deeper analysis of the dynamical system in Sects. 4 and 5.

In phase 1 of the experiment, the baby and the mobile are not coupled ($c = 0$) and the baby performs spontaneous kicks with a rate of about 10 per minute. For the model, this means that the baby oscillator (9) is a pure van-der-Pol that

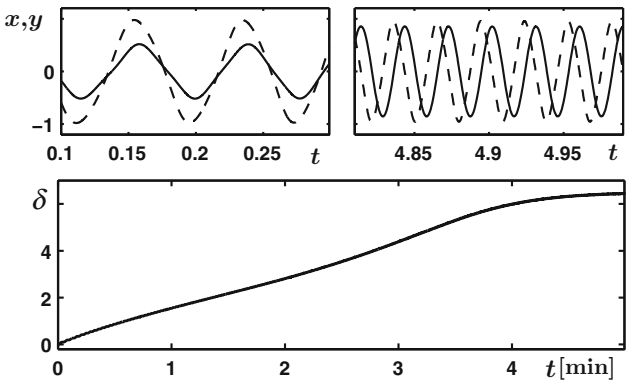

Fig. 2 First part of phase 2: The system is in a positive feedback loop. The driving of y leads to an increases in δ (*lower part*), which increases the frequency of x. Faster driving leads to a larger amplitude in y and a further increase in δ. Initially, the two oscillators are close to in phase (*upper left*; baby *dashed*, mobile *solid*). When the steady state is approached, their phase shift is about 90° (*upper right*). Parameters: $\gamma = -0.25$, $\alpha = 1$, $\omega_0 = 0.6$, $\epsilon = 1$, $\Omega_0 = 2.2$, $c = 2$, $a = 0.18$

oscillates at its basic frequency ω_0 and the mobile and δ are at their resting states $y = \delta = 0$. In the experiment, this phase has a duration of 3 min.

For the simulation, the following parameters were used: $\gamma = -0.25$, $\alpha = 1$, which leads to a stable limit cycle representing the baby's kicks with a peak amplitude $x_m = 2r = 1$. As $\delta = 0$ during this phase, the angular velocity is given by $\omega_0 = 0.6$, and due to $c = 0$, there is no coupling rendering the other parameters irrelevant at this point.

After a delay of 2 min during which a cord was looped around the baby's left ankle and hooked to the suspension bar of the mobile, phase 2 starts where each kick of the baby causes movement in the mobile. Even though there are no quantitative measures of the mobile movement nor any estimates of force produced, it is stated in Rovee and Rovee (1969, p. 35): "... it was apparent that the variety of figure movement increased directly with the force or rate of response. Very rapid responding produced auditory feedback from colliding wooden figures, such that *effectively* more intense responding produced a more intense reward." As a consequence, during a period of about 5 min the kicking rate increased monotonically, saturating at 30–40 kicks per minute, 3 to 4 times the uncoupled rate. We conclude from the above statement that at this point the mobile oscillator is close to resonance.

In the model, this part of phase 2 is shown in Fig. 2, with the kicks, $x(t)$, dashed and the mobile movement, $y(t)$, as solid lines in the upper half. The left part shows a time early in phase 2 ($t = 0.1-0.3$ min). With $c = 2$, the two oscillators in (9) and (10) are now coupled and y is driven by the periodic force x. With $\Omega_0 = 2.2$, $\omega_0 = 0.6$ and $\epsilon = 1$, initially the system is far from resonance and both oscillators are almost in phase at this stage. As the mobile oscillations y^2 are a

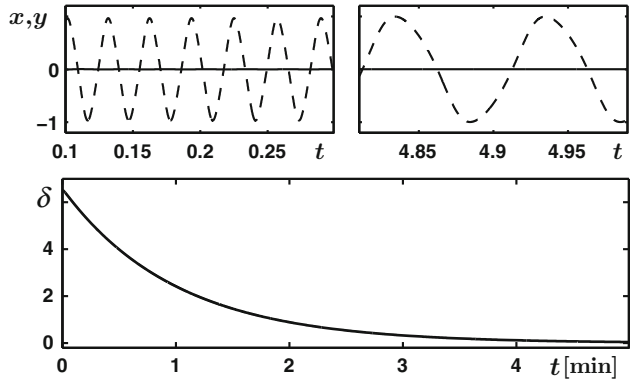

Fig. 3 Phase 3: Baby and mobile, i.e., x and y are no longer coupled and the system returns to its initial state. *Upper part*: Baby (*dashed*) and mobile (*solid*) oscillator at the beginning (*left*) and end (*right*) of phase 3. *Lower part*: Decay of δ. Parameters: Same as in Fig. 2, except $c = 0$

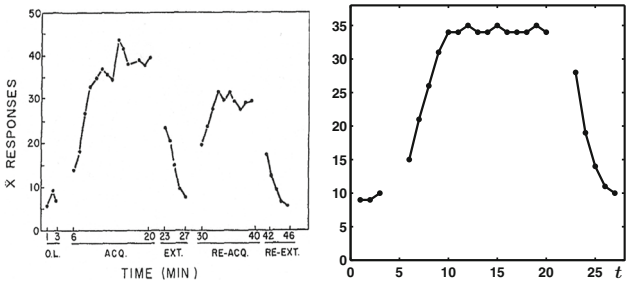

Fig. 4 *Left* Rovee and Rovee (1969) presented their experimental findings as number of kicks in a given minute. *Right* Representation of the model results in the same way. Here, the *dots on the lines* are the number of maxima of the baby oscillator in that minute

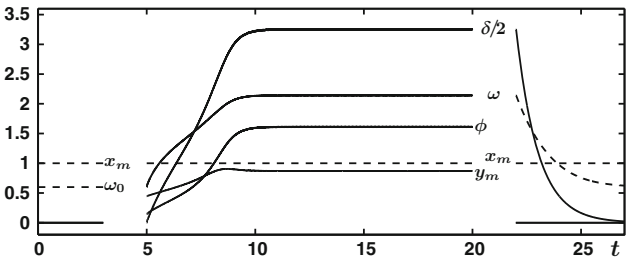

Fig. 5 Model quantities over the entire trial: Amplitudes x_m and y_m, angular velocity ω, $\delta/2$ and the relative phase ϕ

positive input ($a = 0.18$) to the dynamics in (11), δ is driven away from its initial fixed point toward positive values. Now a positive feedback loop starts: The increase in δ feeds into x; i.e., the kicking rate increases. The faster frequency feeds into the mobile y, and, as y oscillates at the driver's frequency, its rate also increases. This leads to a larger amplitude in y because the mobile gets closer to resonance, which increases δ even further. The frequency of x, the amplitude of y and the value of δ saturate when the frequencies of x and y are close to ω_m, i.e., when the system is near resonance. In addition, the bigger the value of δ, the more important the decay term, $-\kappa\delta$, in (11) becomes and an equilibrium is reached. The right upper part in Fig. 2 corresponds to a time about 5 min into phase 2, the time it takes the babies in the experiment to reach their maximum kick rate. The system is close to resonance, and the phase shift between the oscillators is about 90°.

The lower box of Fig. 2 shows the monotonic increase in δ during the first 5 min of phase 2. The second part of phase 2, roughly 10 min long, is a steady-state process. The frequencies and amplitudes of the oscillators as well as the value of δ remain constant.

After about 15 min of the baby being connected to the mobile, the ribbon is removed in a 2-min period after which phase 3 starts. Now the baby can no longer trigger movements of the mobile and within about 5 min the kicking rate decreases to the initial level observed during phase 1. The dynamics of x, y and δ during phase 3 is shown in Fig. 3.

The results in Rovee and Rovee (1969) are plotted in Fig. 4 (left) as the number of kicks counted in a given minute during the 27 min of each trial. In the model, this corresponds to the number of maxima of the baby oscillator in a given time interval. The result from the simulation in this representation is shown in Fig. 4 (right) and is in good agreement with the experiment.

Figure 5 shows the dynamics of all model parameters and quantities over an entire trial.

3.5 Parameters

Most of the parameters are determined by the experimental findings. Three degrees of freedom, the amplitudes of the two oscillators and time, can be chosen arbitrarily. The peak amplitude of the baby oscillator is given by

$$x_m = 2r = 2\sqrt{-\frac{\gamma}{\alpha}} \quad \text{with} \quad \begin{cases} \gamma = -0.25 \\ \alpha = 1 \end{cases} \rightarrow x_m = 1 \tag{12}$$

The frequencies ω_0 and ω_m represent the lower and upper kicking rates of about 10 and 30 kicks per minute, respectively. With $\omega_0 = 0.6$ and $\omega_m = 2$, we find for the kicking rates

$$\nu_l = \frac{100 * 0.6}{2\pi} = 9.6 \quad \text{and} \quad \nu_u = \frac{100 * 2}{2\pi} = 31.8 \tag{13}$$

kicks per minute, where our minute has 100 s, which defines the unit of time. The frequency of the mobile oscillator Ω_0 is then determined from (6)

$$\Omega_0 = \sqrt{\omega_m^2 + \frac{1}{2}\epsilon^2} \tag{14}$$

where ω_m is the frequency we target. Eventually, the oscillators will not be exactly at this rate as their ω also depends on the ratio of κ and a.

During phase 3 the mobile is at rest; i.e., y^2 vanishes and δ falls off exponentially according to

$$\dot{\delta} = -\kappa\delta \quad \rightarrow \quad \delta(t) = \delta_m e^{-\kappa t} \tag{15}$$

which leads to $\kappa \approx 0.01$ to be in agreement with the experiment.

The peak amplitude for the mobile is given by

$$y_m^2 = \frac{c^2 x_m^2}{(\Omega_0^2 - \omega^2)^2 + \epsilon^2\omega^2} \tag{16}$$

For the steady state during phase 2, the system is close to resonance and the first term in the denominator, $(\Omega_0^2 - \omega^2)^2$, is much smaller than $\epsilon^2\omega^2$ and can be neglected, which simplifies the amplitude around resonance

$$y_m \approx \frac{c x_m}{\epsilon\omega_m} \stackrel{!}{=} 1 \quad \rightarrow \quad c = \epsilon\omega_m x_m = 2\epsilon \tag{17}$$

The damping of the mobile oscillator, ϵ, is an interesting parameter because it is a physical quantity that can be easily manipulated. The parameter a may be conceived as an attention parameter (see Sect. 7). κ and a are mainly fixed by the rise and fall times in the model (cf. Fig. 5). We postpone further discussion of the interrelations among these parameters until Sect. 5.

4 Further analysis of the model

To further analyze the properties of the model, we replace the oscillating driving force $y^2(t)$ in (11) by its mean value over one period $\overline{y^2}$. Moreover, we assumed for the parameter estimation in the previous section that the amplitude of the baby oscillator is independent of its frequency (as it is the case for a pure van-der-Pol) and that the driving of the mobile oscillator is sinusoidal. That the latter is not exactly the case is evident from the phase space plots in Fig. 6, which shows strong nonlinear features for the baby oscillator.

To this end, we calculated the oscillator frequencies and amplitudes as well as $\overline{y^2} \approx y_m^2/2$ and the relative phase ϕ as functions of δ from the model analytically and from a numerical simulation. The results are shown in Fig. 7 with the numerical results shown as solid lines and the analytical dependence as dashed lines.

The baby oscillator exhibits a slight dependence of its amplitude x_m on frequency, but the difference from a constant amplitude is small enough to be neglected. The angular velocity ω is expected to increase with δ as

$$\omega = \sqrt{\omega_0^2 + 3\delta r^2} \tag{18}$$

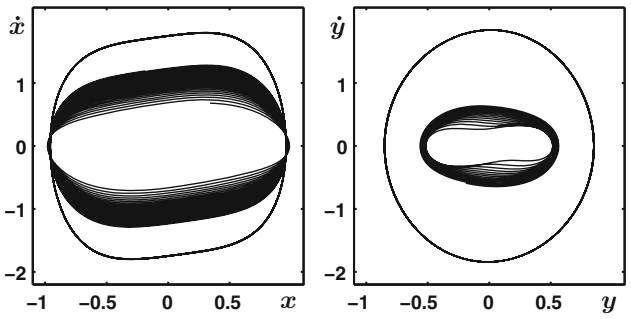

Fig. 6 Phase space plots of the baby (*left*) and mobile (*right*) oscillators during the first 2 min of phase 2 and during the steady state (*inner* and *outer* trajectories, respectively)

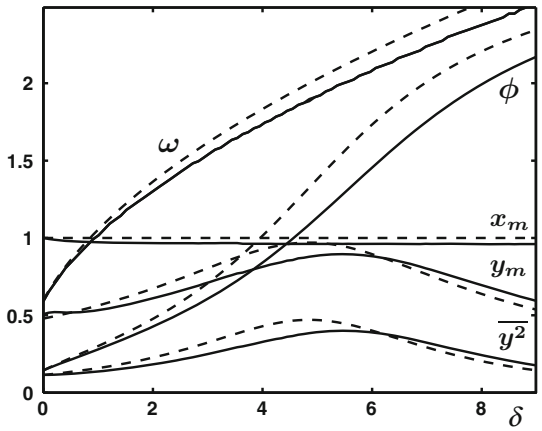

Fig. 7 Comparison of analytical (*dashed*) and numerical (*solid*) dependence of the oscillators' amplitudes (x_m and y_m), frequency ω, mean of the square of $y(t)$ over one period $\overline{y^2}$ and phase shift between the oscillators, ϕ, on δ for $\epsilon = 1$

but increases slower in the numerical simulation. This difference leads to a shift in the resonance curves for y_m and $\overline{y^2}$. In addition, y_m does not reach a maximum of $y_m = 1$, and consequently, the maximum of $\overline{y^2}$ is also smaller in the numerical simulation than expected from the idealized model. Within the parameter range of relevance here, these discrepancies can be compensated with two correction factors for δ and y_m, namely

$$\delta^{(n)} = 0.87\,\delta^{(a)} \quad \text{and} \quad y_m^{(n)} = 0.93\,y_m^{(a)} \tag{19}$$

where the superscripts (n) and (a) correspond to numerical and analytical, respectively. After these corrections, the numerical and analytical dependencies are in good agreement as shown in Fig. 8.

5 Transitions and criticality in the model

By using the average $\overline{y^2}$ in (11), the dynamics of δ can be analyzed independent of the other two equations. We find for the fixed points

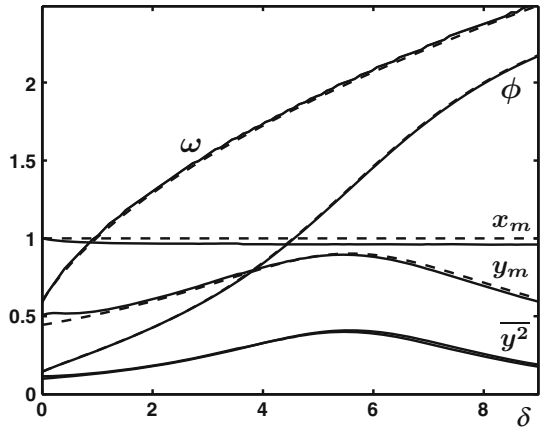

Fig. 8 Same as Fig. 7 with the correction factors applied to δ, y_m and $\overline{y^2}$

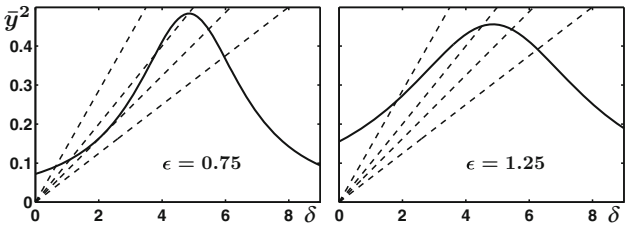

Fig. 9 Fixed points from (22) as intersections between straight lines with slopes κ/a and the resonance curve for values of ϵ below (*left*) and above (*right*) a critical value ϵ_c. In the first case, the system can have one, two or three fixed points, whereas in the second case only one intersection is possible

$$\dot{\delta} = a\overline{y^2} - \kappa\delta = 0 \quad \rightarrow \quad \delta = \frac{a}{\kappa}\overline{y^2} \tag{20}$$

with

$$\overline{y^2} = \frac{1}{2}\frac{(2rc)^2}{(\Omega_0^2 - \omega^2)^2 + \epsilon^2\omega^2} = \frac{2r^2c^2}{(\Omega_0^2 - \omega^2)^2 + \epsilon^2\omega^2} \tag{21}$$

The fixed points are given by the intersection of a straight line through the origin and the resonance curve

$$\frac{\kappa}{a}\delta = \frac{2r^2c^2}{(\Omega_0^2 - \omega^2)^2 + \epsilon^2\omega^2} \tag{22}$$

where the right-hand side depends on δ because

$$\omega^2 = \omega_0^2 + 3\delta r^2 \tag{23}$$

Depending on the damping parameter ϵ, we find two qualitatively different regions, where for small values of ϵ the system can have one, two of three fixed points depending on a, whereas above a critical value ϵ_c only a single intersection is possible as shown in Fig. 9.

The fixed points can be calculated from (22), which is a cubic equation in δ and reads explicitly

$$9r^4\delta^3 - 6r^2\{\Omega_0^2 - \omega_0^2 - \frac{1}{2}\epsilon^2\}\delta^2 + \left\{(\Omega_0^2 - \omega_0^2)^2 + \epsilon^2\omega_0^2\right\}\delta - \frac{2ar^2c^2}{\kappa} = 0 \tag{24}$$

For (24) to have three real solutions, it is necessary (but not sufficient) that its derivative

$$27r^4\delta^2 - 12r^2\left\{\Omega_0^2 - \omega_0^2 - \frac{1}{2}\epsilon^2\right\}\delta + (\Omega_0^2 - \omega_0^2)^2 + \epsilon^2\Omega_0^2 = 0 \tag{25}$$

has two real solutions corresponding to a maximum and minimum given by

$$\delta_{1,2} = \frac{1}{9r^2}\left\{2(\Omega_0^2 - \omega_0^2 - \frac{1}{2}\epsilon^2) \pm \sqrt{(\Omega_0^2 - \omega_0^2)^2 + \epsilon^2(\omega_0^2 - 4\Omega_0^2) + \epsilon^4}\right\} \tag{26}$$

For the critical ϵ, the discriminant in (26) has to vanish so that there is only a single real solution, i.e., the minimum and maximum collide, leading to an inflection point with a horizontal tangent. The critical ϵ as a function of Ω_0^2 and ω_0^2 is therefore given by

$$\epsilon_{1,2}^2 = \frac{1}{2}\left\{4\Omega_0^2 - \omega_0^2 \pm \sqrt{12\Omega_0^4 - 3\omega_0^4}\right\} \tag{27}$$

In our model, the frequency of the mobile oscillator Ω_0 depends on ϵ

$$\Omega_0^2 = \omega_m^2 + \frac{1}{2}\epsilon^2 \tag{28}$$

Inserting (27) into (28) and solving for ϵ leads to one meaningful, i.e., positive value for the critical parameter

$$\epsilon_c^2 = -2\omega_m + \frac{2\sqrt{3}}{3}\sqrt{4\omega_m^4 + \omega_0^4 - 2\omega_m^2\omega_0^2} \quad \rightarrow \quad \epsilon_c \approx 1.0183 \tag{29}$$

as a function of ω_0 and ω_m and the numerical values used before.

The dynamics of (20) for the damping parameter ϵ below, at and above its critical value ϵ_c is summarized in Figs. 10, 11 and 12. On the left are phase space plots with the function (24), where intersections with the horizontal line with a negative slope indicate δ values that are stable fixed points (attractors), whereas intersections with a positive slope represent unstable fixed points (repellers). In the middle the resonance curves and their intersections with the lines $\kappa\delta/a$ are shown, and on the right are the temporal dynamics of δ during the first 10 min of phase 2.

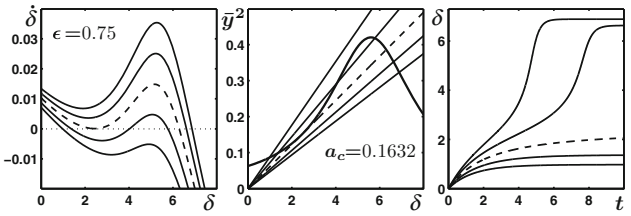

Fig. 10 Dynamical properties for $\epsilon = 0.75 < \epsilon_c$ for the critical value of a (*dashed*) as well as 0.02 and 0.04 above and below a_c (*solid*). *Left* Phase space plots $\dot{\delta}$ as a function of δ. There is a critical value a_c where the system has two fixed points, separating parameter regions with three and a single fixed point. *Middle* Fixed points as intersections of straight lines with slope κ/a with the resonance curve. *Right* Temporal dynamics of δ during the first 10 min of phase 2

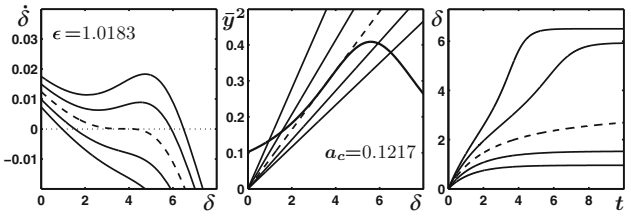

Fig. 11 Same as Fig. 10 for $\epsilon = 1.0183 = \epsilon_c$

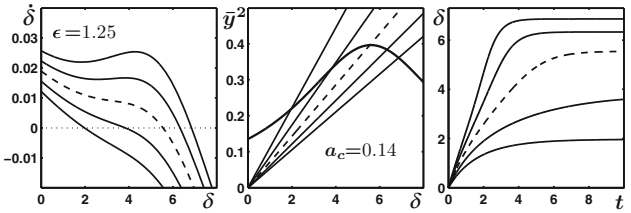

Fig. 12 Same as Fig. 10 for $\epsilon = 1.25 > \epsilon_c$. In this case, there is no critical a and a_c indicates the value for which the intersection occurs at resonance

For values of $\epsilon < \epsilon_c$, there is a critical value a_c that separates parameter regions where one or three fixed points exist. For values of $a < a_c$, the system reaches a stationary state below the inflection point of the resonance curve. This means that when a is low, δ is small and the kick rate does not increase much. Only for $a > a_c$ does the system enter a state close to resonance where kicking rates can triple. The dynamics of δ during the transient part of phase 2 speeds up considerably before the steady state is reached.

For damping parameters at or above ϵ_c, there is only one fixed point in the system but remnants of the other two are still visible in the phase space plot and the δ-dynamics for damping values close to ϵ_c.

The dynamics of δ described by (20) can be derived from a potential function

$$\dot{\delta} = a\overline{y^2} - \kappa\delta = -\frac{\mathrm{d}V(\delta)}{\mathrm{d}\delta} \tag{30}$$

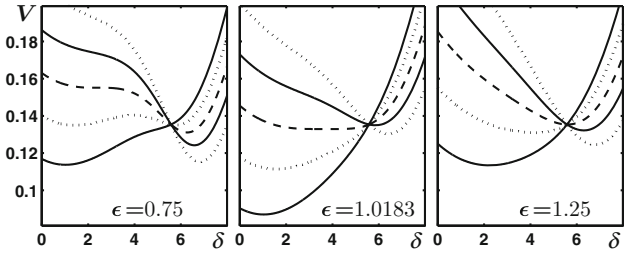

Fig. 13 Potential functions V(δ) from (32) for ϵ below (*left*) at (*middle*) and above (*right*) the critical value. Functions are shown for a_c (*dashed*) and 0.02 and 0.04 above and below this value. *Dotted lines* are used to make it easier to follow them through the common intersection

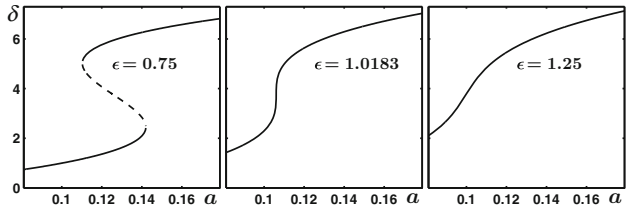

Fig. 14 Bifurcation diagrams: The fixed points for δ as a function of a for ϵ below (*left*) at (*middle*) and above (*right*) the critical value. Stable fixed points (attractors) are indicated by *solid lines*, and *dashed lines* correspond to unstable points (repellers). For $\epsilon < \epsilon_c$, the system shows hysteresis

with

$$\begin{aligned} V(\delta) &= -\int \left\{ \frac{2ar^2c^2}{n(\delta)} - \kappa\delta \right\} \mathrm{d}\delta \\ n(\delta) &= 9r^4\delta^2 - 6r^2 \left\{ \Omega_0^2 - \omega_0^2 - \frac{1}{2}\epsilon^2 \right\} \delta \\ &\quad + (\Omega_0^2 - \omega_0^2)^2 + \epsilon^2\omega_0^2 \end{aligned} \tag{31}$$

Explicitly, the potential takes the form

$$\begin{aligned} V(\delta) &= \frac{2ac^2}{3\epsilon\sqrt{\Omega_0^2 - \frac{1}{4}\epsilon^2}} \\ &\quad \times \arctan \left\{ \frac{3r^2\delta - (\Omega_0^2 - \omega_0^2 - \frac{1}{2}\epsilon^2)}{\epsilon\sqrt{\Omega_0^2 - \frac{1}{4}\epsilon^2}} \right\} + \frac{1}{2}\kappa\delta^2 \end{aligned} \tag{32}$$

The potential functions (32) are shown in Fig. 13 for ϵ below, at and above ϵ_c for five values at and around a_c.

In Fig. 14, bifurcation diagrams for δ as functions of the parameter a are shown. For $\epsilon < \epsilon_c$, the system exhibits hysteresis. For $\epsilon < \epsilon_c$, there is a threshold for a: When a is below that threshold only small kicking rates can be reached and only above a_c can the large kicking rates seen experimentally occur. This is the discontinuity that leads to hysteresis in the

model. Above ϵ_c (Fig. 14, right) there is a continuum with larger a meaning faster kicks.

6 Model predictions

As mentioned above, a critical value for the damping constant of the mobile, ϵ_c, separates two parameter régimes where the dynamics is monostable or bistable. As Fig. 14 (left) shows, for small damping a critical value a_c of the attention parameter must be reached for the baby to realize it is causing the motion of the mobile. If a single kick already sets the mobile in motion there is no need to kick beyond the spontaneous rate to keep it going. Moreover, it is probably crucial for the "eureka effect" that every kick leads to a substantial change in the mobile that the baby can detect as causing its motion. A manipulation of the damping characteristic of the mobile is therefore an important test for the model. Another quantity that can be manipulated experimentally is the resonant frequency of the mobile in relation to the baby's kick rate. Does the baby adjust its kick rate to the resonant frequency of the mobile? If so, since fast kicks produce a smaller response, a low resonant frequency should trigger a slower kicking rate. Our model, basically a three-dimensional dynamical system for the key components with a single bifurcation parameter, ϵ, reproduces the MCR phenomenon. Although more detailed data on individual trials on individual babies would be of considerable interest to compare with predictions of our model (cf. Fig. 5 and Sect. 5), the overall picture on infant kick rate is captured quite nicely (cf. Fig. 4).

How the coupling between baby and mobile affects the baby's behavior and sense of agency is an open issue. Instead of a ribbon or tether, Chen et al. (2002) used a touch pad that when contacted by the baby's foot triggered mobile movement. Recent work by Sargent et al. (2014) used a "virtual threshold," individualized to each baby's spontaneous kicking action, that when crossed activated the mobile. Although the baby's sense of its own movement is crucial to produce MCR, enhanced tactile and kinesthetic information through the tension on the tether does not appear to be mandatory. As long as the baby detects that through his or her *own* movements he or she is causing the mobile to move, it does not appear to matter how the baby is coupled to the mobile. It may well be, however, that certain forms of coupling are more effective than others. As of now, our model predicts that bidirectional coupling between baby and mobile movement is crucial; the form that coupling takes, e.g., in terms of creating an optimal infant/environment interface needs further study. Finally, it is clear that after baby and mobile motion are decoupled, the baby's movements take some time to return to their baseline rate. This suggests that as a result of making the mobile move, expectations are created in an if/then mode; i.e., if I continue to kick then this will cause the mobile to move. The conditions under which such expectations are created and the time scales of their demise, i.e., the κ parameter are worth exploring.

7 Discussion

Conjugate reinforcement is a term that stems from the tradition of operant conditioning: It has been dubbed the most "fundamental schedule" in that field because it parallels our perceptions and interactions with nature. A remarkable feature of mobile conjugate reinforcement (MCR) is that within minutes, infants recognize the correspondence between their own movements and the motion of the mobile. This robust behavioral phenomenon has been used not only as a window into the processes of infant learning, remembering and forgetting (for review Rovee-Collier et al. 1980; Mullally and Maguire 2014) but also as a means to understand basic aspects of motor development (Kelso and Clark 1982; Thelen and Smith 1994) including topographical response differentiation (Angulo-Kinzler 2001; Rovee-Collier et al. 1978) and the transition from spontaneous to instrumental behavior (Sargent et al. 2014; Thelen and Fisher 1983). Although the infant–mobile interaction is clearly co-regulated, all the studies to date have focused analysis on the baby and may be said to be "organism-centric": The only aspects measured are the number of kicks or "motor units" (Thelen 1994) produced over a given interval of time in response to the stimulus. Theoretically, the coordination between neuromuscular and perceptual activities is deemed to be crucial for development (Lewis 2000; Thelen and Smith 1994), but the relationship between baby movement and mobile motion is never quantified. Here, using the concepts, methods and tools of coordination dynamics we provide a model that accounts for not just what babies do (such as increase the rate of kicking or alter leg movement patterns), but offers an underlying dynamical mechanism based on the role the mobile plays and the joint pattern of interaction or functional coupling between baby and mobile.

A most remarkable aspect of MCR is that the baby—capable of producing spontaneous leg movements—rapidly realizes that it, not some outside force, is moving the mobile. A switching or kind of "eureka effect" occurs between spontaneous and intentional movement. The faster the baby kicks, the more vigorously the mobile will move. This conjugate arrangement leads to a high and stable rate of leg movement, which subsides only when the ribbon is detached. Such contingent control of the mobile appears to be highly reinforcing (of high "value" in modern parlance) and appears to depend on both response rate and amplitude. Rovee-Collier and Gekoski (1979) report that depending on response rate, the inertial properties, essentially the damping of the mobile,

permit recurrent kicks to drive the intensity of mobile movements up to some (unmeasured) point of activation.

The key mechanism in the model underlying the eureka-like phase transition is positive feedback: A spontaneous "kick" moves the mobile, the perceptual consequences of which lead to more forceful kicks and a (tripling) increase in the kick rate. In this respect, evidence suggests that the baby's attention to self-generated movements and the kinesthetic, visual and auditory consequences they produce is a crucial factor. In our model, if this parameter is below a critical threshold, kick rate does not increase much. Only above a critical value of a does the kick rate increase to around triple the baseline level. This feature of the model at the level of individual trials is obviously open to testing. High arousal and sustained visual attention accompanied by open arm up and down motions along with fast leg movements is known to peak in infants around 9–12 weeks. Interestingly, in other contexts that involve mutual coupling, this kind of "excited attention" on the part of the infant affects the occurrence of maternal affectionate talking which is also bidirectionally linked to infant smiling (Lavelli and Fogel 2013). Although not modeled as such, positive feedback appears to be an essential mechanism not just for MCR but also for normal communication patterns and the secure attachment of mother and infant. Our model is reminiscent of theories of pattern formation in development (Gierer and Meinhardt 1972; Meinhardt 1982) that stress the joint factors of positive feedback (autocatalysis or "self-enhancement") and inhibition (here represented by κ, which limits the increase in kicking). Likewise, our model is compatible with the "feed-forward loop" network motif, so ubiquitous in biological circuits (Alon 2007). It is intriguing to think that the same principles shown here to govern an essential aspect of infant behavior may apply also to biological development in general. Detailed modeling of recurrent networks composed of excitatory and inhibitory neuron layers in primary visual cortex suggests that both highly structured visual input and intrinsic spontaneous activity drive the learning of synapses to produce direction selective neurons. Interestingly, Wenisch et al. (2005) demonstrate that spatiotemporal tuning of synapses via an asymmetric coupling structure is capable of producing maps of direction preference much like those found in optical imaging studies. Their principle of direction selective neuronal responses based on asymmetric coupling of inputs within a neuron's integration field provides a promising basis for learning by spike-timing-dependent plasticity: Coupling strengths within the integration field may be modified when learning is driven by an activity wave such as would be produced by a moving mobile.

The fact that MCR involves complex coordinated behavior in which highly complex "stimuli" are linked to time-locked movement suggests a transition from quasi-random to more periodic movements, a kind of "disorder" to "order" transition. That the leg drives the mobile and that mobile and leg movements become synchronized may relate to other examples in nature ranging from fireflies, to "pacemaker" neurons and locust flight pattern generators (see Kelso et al. 1990). Thus, MCR may fall under the more general principles of coordination and entrainment. Once the infant realizes it is causing the mobile to jiggle, information from various modalities must be integrated for the task at hand. Although the ribbon is a physical connection, the coordination observed in MCR is clearly informational and presumably relies on an intact nervous system. In this regard, although we know quite a lot about the neural circuitry (DeLuca et al. 2010; Jantzen et al. 2004) and dynamics (Kelso et al. 1998; Mayville et al. 2002) involved in simple synchronization and syncopation tasks, developmental research using fMRI is at a very early stage (Mullally and Maguire 2014). Combining MCR with modern brain imaging methods is thus highly desirable. As in the case of modeling the brain dynamics of bimanual and sensorimotor coordination (Jirsa et al. 1998; Fuchs et al. 2000; Kelso et al. 2013; see also Rabinovich et al. 2012), this opens up the possibility to make direct connections between our theoretical model of MCR and its neurophysiological counterparts.

Finally, we note that whereas MCR has been recognized as an impressive example of the infant's ability to control, learn and remember, we draw attention to the deeper issue of the origins of self-motion[2]. On first blush, the present model suggests an interpretation of mobile conjugate reinforcement in which synergetic self-organization, the spontaneous formation and change of patterns in open, nonequilibrium systems (Haken 1978, 1983)—here instantiated in the spontaneous kicking movements of prelinguistic infants—gives rise to agency (Kelso 2002). While recognizing the significance of spontaneous self-organizing processes, the present analysis goes a step further. It says that the sense of self emerges as an explicitly *collective effect* spanning baby and mobile movement, a meaningful context-specific relation between the organism and its environment. In more exacting terms, the sense of agency amounts to the "eureka" experience of making something happen in the world, a near magical combination of animate and inanimate movement.

Acknowledgments We wish to express our gratitude to Maxine Sheets-Johnstone for her inspirational and insightful writings on animate movement and for her encouraging comments on this work. Thanks also to an anonymous reviewer and the Editor, Leo van Hemmen, for helpful comments that improved the MS. The research was supported by a grant from the US National Institute of Health (MH080838), the Chaire d'Excellence Pierre de Fermat and the FAU Foundation (Eminent Scholar in Science). Preliminary versions of the paper were presented by JASK at the 18th Herbstakademie on "The

[2] We are reminded of Newton's words in a letter to Oldenburg in 1675: "self-motion," Newton remarked, "is beyond our understanding" (cited in Gleick 2003, p. 105).

Circularity of Mind and Matter," Heidelberg, Germany, March 26–27, 2015, and the 110th Meeting of The Society of Experimental Psychologists, Charlottesville, VA, April 17–18, 2015.

References

Ajallooeian M, van den Kieboom J, Mukovskiy A, Giese M, Ijspeert A (2013) A general family of morphed nonlinear phase oscillators with arbitrary limit cycle shape. Physica D 262:41–56

Alon U (2007) An introduction to systems biology: design principles of biological circuits. Chapmann & Hall/CRC, Boca Raton

Angulo-Kinzler RM (2001) Exploration and selection of intralimb coordination patterns in 3-month-old infants. J Motor Behav 33:363–376

Angulo-Kinzler RM, Ulrich B, Thelen E (2002) Three-month-old infants can select specific leg motor situations. Motor Control 6:52–68

Assisi CG, Jirsa VK, Kelso JAS (2005) Dynamics of multifrequency coordination using parametric driving: theory and experiment. Biol Cybern 93:6–21

Bardy BG, Marin L, Stoffregen TA, Bootsma RJ (1999) Postural coordination modes considered as emergent phenomena. J Exp Psychol Human 25:1284–1301

Beek PJ, Schmidt RC, Sim MY, Turvey MT (1995) Linear and nonlinear stiffness and friction in biological rhythmic movements. Biol Cybern 73:499–507

Beek PJ, Rikkert WEI, van Wieringen PCV (1996) Limit cycle properties of rhythmic forearm movements. J Exp Psychol Human 22:1077–1093

Beek PJ, Peper L, Daffertshofer A (2002) Modeling rhythmic interlimb coordination: beyond the Haken-Kelso-Bunz model. Brain Cogn 48:149–165

Buchanan JJ, Kelso JAS, Fuchs A (1996) Coordination dynamics of trajectory formation. Biol Cybern 74:41–54

Chemero A (2011) Radical Embodied cognitive science. MIT Press, Cambridge

Chen Y, Ding M, Kelso JAS (1997) Long term memory processes ($1/f^{\alpha}$) in human coordination. Phys Rev Let 79:4501–4504

Chen YP, Fetters L, Holt KG, Saltzman E (2002) Making the mobile move: constraining task and environment. Infant Behav Dev 25:195–220

DeGuzman GC, Kelso JAS (1991) Multifrequency behavioral patterns and the phase attractive circle map. Biol Cybern 64:485–495

DeLuca C, Jantzen KJ, Comani S, Bertollo M, Kelso JAS (2010) Striatal activity during intentional switching depends on pattern stability. J Neurosci 30:3167–3174

Dumas G, DeGuzman GC, Tognoli E, Kelso JAS (2014) The human dynamic clamp as a paradigm for social interaction. Proc Natl Acad Sci 111:E3726

Edelman GM (1987) Neural Darwinism: the theory of neural group selection. Basic Books, New York

Eisenhammer T, Hübler A, Packard N, Kelso JAS (1991) Modeling experimental time series with ordinary differential equations. Biol Cybern 65:107–112

Fink PW, Kelso JAS, DeGuzman GC (2000) Recruitment of degrees of freedom stabilizes coordination. J Exp Psychol Human 26:671–692

Fink PW, Kelso JAS, Jirsa VK (2009) Perturbation-induced false starts as a test of the Jirsa-Kelso excitator model. J Mot Behav 41:147–157

Fuchs A (2013) Nonlinear dynamics in complex systems. Springer, Berlin

Fuchs A, Jirsa VK (eds) (2008) Coordination: neural behavioral and social dynamics. Springer, Berlin

Fuchs A, Jirsa VK, Kelso JAS (2000) Theory of the relation between human brain activity (MEG) and hand movements. Neuroimage 11:359–369

Gierer A, Meinhardt H (1972) A theory of biological pattern formation. Kybernetik 12:30–39

Gleick J (2003) Isaac Newton. Pantheon Books, New York

Haken H (1978) Synergetics. An introduction. Springer, Berlin

Haken H (1983) Advanced synergetics. Springer, Berlin

Haken H, Kelso JAS, Bunz H (1985) A theoretical model of phase transitions in human hand movements. Biol Cybern 51:347–356

Haken H, Kelso JAS, Fuchs A, Pandya A (1990) Dynamic pattern recognition of coordinated biological motion. Neural Netw 3:347–356

Howard IS, Ingram JN, Kording KP, Wolpert DM (2009) Statistics of natural movements are reflected in motor errors. J Neurophysiol 102:1902–1910

Huys R, Perdikis D, Jirsa VK (2014) Functional architectures and structured flows on manifolds: a dynamical framework for motor behavior. Psychol Rev 121:302–336

Ijspeert A, Grillner S, Dario P (2013a) Foreword for the special issue on lamprey and salamander robots and the central nervous system. Biol Cybern 107(5):495–496

Ijspeert A, Nakanishi J, Hoffmann H, Pastor P, Schaal S (2013b) Dynamical movement primitives: learning attractor models for motor behaviors. Neural Comput 25:328–373

Jantzen KJ, Steinberg FL, Kelso JAS (2004) Brain networks underlying timing behavior are influenced by prior context. Proc Natl Acad Sci USA 101:6815–6820

Jeka JJ, Kelso JAS, Kiemel T (1993) Pattern switching in human multilimb coordination dynamics. Bull Math Biol 55:829–845

Jensen JL, Thelen E, Ulrich BD (1989) Constraints on multijoint movements: from the spontaneity of infancy to the skill of adults. Hum Mov Sci 8:393–402

Jirsa VK, Kelso JAS (2005) The excitator as a minimal model for the coordination dynamics of discrete and rhythmic movements. J Motor Behav 37:35–51

Jirsa VK, Fuchs A, Kelso JAS (1998) Connecting cortical and behavioral dynamics: bimanual coordination. Neural Comput 10:2019–2045

Kay BA, Kelso JAS, Saltzman EL, Schöner G (1987) Space-time behavior of single and bimanual rhythmical movements: data and limit cycle model. J Exp Psychol Human 13:178–192

Kay BA, Saltzman EL, Kelso JAS (1991) Steady-state and perturbed rhythmical movements: a dynamical analysis. J Exp Psychol Human 17:183–197

Kelso JAS (1981) On the oscillatory basis of movement. Bull Psychon Soc 18:63

Kelso JAS (1984) Phase transitions and critical behavior in human bimanual coordination. Am J Physiol 246:R1000–R1004

Kelso JAS (1995) Dynamic patterns: the self organization of brain and behavior. MIT Press, Cambridge

Kelso JAS (2002) The complementary nature of coordination dynamics: self-organization and the origins of agency. Nonlinear Phenom Compl Syst 5:364–371

Kelso JAS (2009) Coordination dynamics. In: Meyers RA (ed) Encyclopedia of complexity and system science. Springer, Berlin, pp 1537–1564

Kelso JAS, Clark JE (eds) (1982) The development of human movement coordination and control. Wiley, New York

Kelso JAS, Haken H (1995) New laws to be expected in the organism: synergetics of brain and behavior. In: Murphy M, O'Neill L (eds) What is life? The next 50 years. Cambridge University Press, Cambridge

Kelso JAS, Holt KG, Rubin P, Kugler PN (1981) Patterns of human interlimb coordination emerge from the properties of nonlinear oscillatory processes: Theory and data. J Motor Behav 13:226–261

Kelso JAS, DelColle J, Schöner G (1990) Action-perception as a pattern formation process. In: Jeannerod M (ed) Attention and performance XIII. Erlbaum, Hillsdale, pp 139–169

Kelso JAS, Fuchs A, Holroyd T, Lancaster R, Cheyne D, Weinberg H (1998) Dynamic cortical activity in the human brain reveals motor equivalence. Nature 392:814–818

Kelso JAS, Dumas G, Tognoli E (2013) Outline of a general theory of behavior and brain coordination. Neural Netw 37:120–131

Kostrubiec V, Zanone PG, Fuchs A, Kelso JAS (2012) Beyond the blank slate: routes to learning new coordination patterns depend on the intrinsic dynamics of the learner - experimental evidence and theoretical model. Front Hum Neurosci 6:1–14

Laughlin RB, Pines D (2000) The theory of everything. Proc Natl Acad Sci 97:28–31

Lavelli M, Fogel A (2013) Interdyad differences in early mother-infant face-to-face communication: real-time dynamics and developmental pathways. Dev Psychol 49:2257–2271

Lewis M (2000) The promise of dynamic systems approaches for an integrated account of human development. Child Dev 71:36–43

Mayville JM, Jantzen KJ, Fuchs A, Steinberg F, Kelso JAS (2002) Cortical and subcortical networks underlying syncopated and synchronized coordination revealed using fMRI. Hum Brain Mapp 17:214–219

Meinhardt H (1982) Models of biological pattern formation. Academic Press, New York

Mullally S, Maguire E (2014) Learning to remember: the early ontogeny of episodic memory. Dev Cogn Neurosci 9:12–29

Perdikis D, Huys R, Jirsa VK (2011) Time scale hierarchies in the functional organization of complex behaviors. PLoS Comp Biol 7(e1002):198

Plenz D, Niebur E (eds) (2014) Criticality in neural systems. Wiley, New York

Port R, van Gelder T (eds) (1995) Mind as motion: explorations in the dynamics of cognition. MIT Press, Cambridge

Rabinovich M, Friston K, Varona P (eds) (2012) Principles of brain dynamics. MIT Press, Cambridge

Raibert MH (1986) Legged robots that balance. Cambridge University Press, Cambridge

Rovee CK, Rovee DT (1969) Conjugate reinforcement of infant exploratory behavior. J Exp Child Psychol 8:33–39

Rovee-Collier C, Gekoski MJ (1979) The economics of infancy: a review of conjugate reinforcement. In: Reese HW, Lipsitt LP (eds) Advances in child development and behavior. Academic, New York, pp 195–255

Rovee-Collier C, Morrongiello BA, Aron M, Kupersmidt J (1978) Topographical response differentiation in three-month-old infants. Infant Behav Dev 1:149–176

Rovee-Collier C, Sullivan MV, Enright M, Lucas D, Fagen JW (1980) Reactivation of infant memory. Science 208:1159–1161

Sargent B, Schweighofer N, Kubo M, Fetters L (2014) Infant exploratory learning: influence on leg joint coordination. PLoS ONE 9(e91):500

Schöner G, Kelso JAS (1988) Dynamic pattern generation in behavioral and neural systems. Science 239:1513–1520

Schöner G, Haken H, Kelso JAS (1986) A stochastic theory of phase transitions in human hand movement. Biol Cybern 53:247–257

Sheets-Johnstone M (2011) The primacy of movement. John Benjamins, Amsterdam

Thelen E (1994) Three-month old infants can learn task-specific patterns of interlimb coordination. Psychol Sci 5:280–285

Thelen E, Fisher DM (1983) From spontaneous to instrumental behavior: kinematic analysis of movement changes during very early learning. Child Dev 54:129–140

Thelen E, Smith LB (1994) A dynamic systems approach to the development of cognition and action. MIT Press, Cambridge

Thelen E, Bradshaw G, Ward JA (1981) Spontaneous kicking in month old infants: manifestations of a human central motor program. Behav Neural Biol 32:45–53

Thelen E, Kelso JAS, Fogel A (1987a) Self organizing systems and infant motor development. Dev Rev 7:39–65

Thelen E, Skala KD, Kelso JAS (1987b) The dynamic nature of early coordination: evidence from bilateral leg movements in young infants. Dev Psychol 23:179–186

Turvey MT, Carello C (2012) On intelligence from first principles: guidelines for inquiry into the hypothesis of physical intelligence (PI). Ecol Psychol 24:3–32

Wenisch OG, Noll J, van Hemmen JL (2005) Spontaneously emerging direction selectivity maps in visual cortex through STDP. Biol Cybern 93:239–247